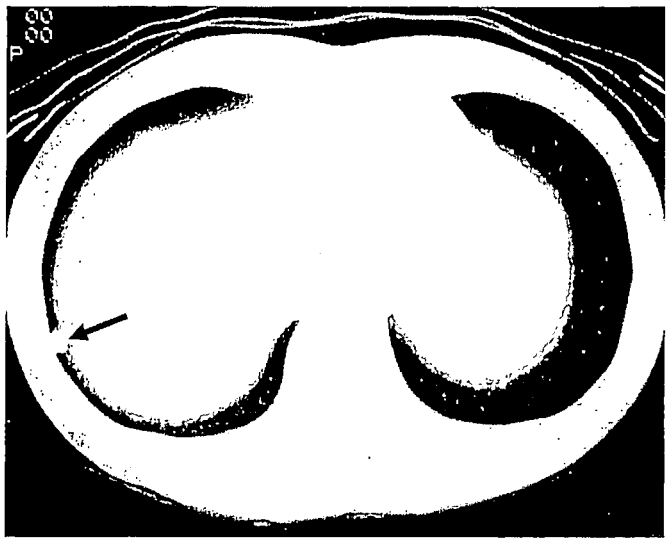

Fig. 1. Case 1.
Computed tomography showing a single lung metastasis (arrow) in the right lower lobe near the pleura.

Fig. 2. Case 1.
The lung metastasis was located in the right lower lobe and was exposed on the visceral pleura (black arrows). The pleural metastasis was noted on the diaphragm which was in the area in contact with the lung metastasis (white arrows).

tastases were resected via thoracoscopy, but there were no pleural tumors at that time. Eighty one months after the first resection of metastases, the patient is alive and has not had a recurrence.

Case 2

An 11-year-old female with femoral osteosarcoma underwent preoperative chemotherapy with CDDP and DXR, followed by an extended resection of the left femur and reconstruction in February 2003. Adjuvant chemotherapy with CDDP and CPA was administered for a total of 10 courses until January 2004. In October 2004, a single lung metastasis was found in the right lower lobe by CT. A needle biopsy was not performed. The thoracoscopy showed a lung metastasis which was located in the right lower lobe which was exposed on the visceral pleura. Precise observation of the intrathoracic wall showed no other tumor on either the parietal or visceral pleura. The tumor was resected, followed by chemotherapy with IFO. The pathological diagnosis of the tumor was metastatic osteosarcoma. In March 2005, a pleural metastasis was found by CT (Fig. 3). The thoracoscopy showed a metastasis, 5.3 cm in size, located at the parietal pleura, within the area which was in contact with the scar of the first metastasectomy (Fig. 4). The pleural metastasis was completely resected with intercostals muscle. The pathological examination showed that the tumor was metastatic osteosarcoma and that it was covered with a fibrous capsule but not by mesothelial epithelium. The patient is now alive without recurrence 3 months after the last surgery.

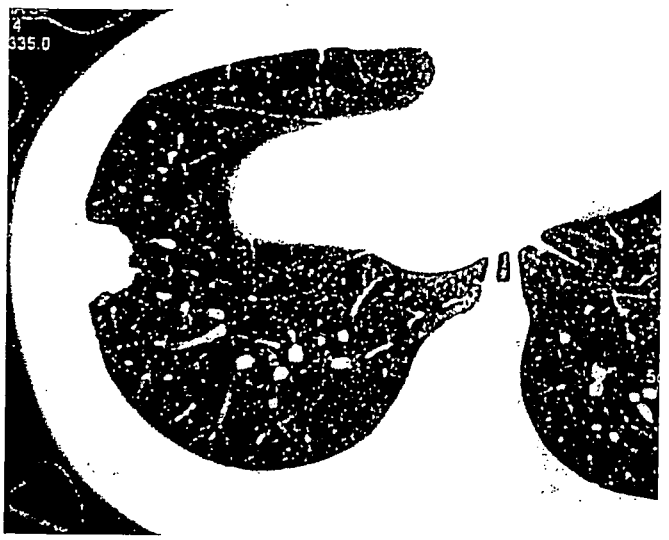

Fig. 3. Case 2.
Computed tomography of the pleural tumor showing extrapleural signs.

A B

Fig. 4. Case 2.
A: The metastatic pleural tumor which was exposed on the surface of the lung at first metastasectomy (arrows).
B: The metastatic pleural tumor (black arrows) was located on the parietal pleura in front of the scar (white arrows) of the first metastasectomy.

Discussion

As far as we have reviewed, pleural metastasis due to contact with a lung metastasis of osteosarcoma has not yet been reported. Although the pleural metastases in these two patients may have been hematogenous, we believe that both pleural metastases occurred as a result of contact with the previous lung metastases for the following reasons: (1) Although the lung metastasis and pleural metastasis were completely separated from each other in both of the two patients, the pleural metastases were within an area in contact with the lung metastasis during ordinary lung expansion in ventilation; and (2) Both the lung and pleural metastases in the two patients were covered with a fibrous capsule but not by mesothelial epithelium; and (3) After resection of the pleural metastasis, the first patient has not suffered another pleural metastasis or dissemination for over 6 years, which could be explained by the pleural metastasis originating from contact with the lung tumor rather than a hematogenous metastasis or a

dissemination. Although we do not entirely deny the possibility of a hematogenous metastasis or dissemination, it can be surmised that the pleural metastasis of osteosarcoma could occasionally originate from a 'kissing metastases' to the pleura near the site of the lung metastasis, as in the present two cases. While patients with lung metastasis from osteosarcoma usually had bloody pleural effusion, pleural metastasis was rarely found with lung metastasis of osteosarcoma, which was contrary to lung metastasis from carcinoma. Although kissing pleural metastases of osteosarcoma have not been reported before, Nomori et al. reported a patient with a kissing metastases of a fibrous tumor of the pleura.[3] We believe that the kissing metastases could also occur in other kinds of intrathoracic neoplasms, especially in sarcoma rather than carcinoma.

Skinner et al. reported that a 5-year survival rate in the patients with pulmonary metastases of osteosarcoma was 41% after metastasectomy and systemic chemotherapy.[4] Because a kissing pleural metastases of osteosarcoma can be cured after complete resection, we conclude that the pleural cavity in contact with the lung metastasis should be thoroughly observed under a thoracoscopy. Whenever a metastasizing pleural tumor is found within the area in contact with the lung metastasis, the lesions and the surrounding pleura should be resected completely, which could improve the prognosis of patients.

References

1. Jeffree GM, Price CH, Sissons HA. The metastatic patterns of osteosarcoma. *Br J Cancer* 1975; **32**: 87–107.
2. Japanese Society of Pathology. Japan Autopsy Annual Database. Tokyo: Japanese Society of Pathology. (in Jpse.)
3. Nomori H, Horio H, Fuyuno G, Morinaga S. Contacting metastasis of a fibrous tumor of the pleura. *Eur J Cardiothorac Surg* 1997; **12**: 928–30.
4. Skinner KA, Eilber FR, Holmes EC, Eckardt J, Rosen G. Surgical treatment and chemotherapy for pulmonary metastases from osteosarcoma. *Arch Surg* 1992; **127**: 1065–71.

Ann Thorac Surg
2006;81:1132–4

Positive Imaging of Thymoma by 11C-Acetate Positron Emission Tomography

Takashi Ohtsuka, MD, Hiroaki Nomori, MD, PhD, Kenichi Watanabe, MD, Tsuguo Naruke, MD, PhD, Keiichi Suemasu, MD, PhD, Noboru Kosaka, MD, PhD, and Kimiichi Uno, MD, PhD

Department of Thoracic Surgery and Saiseikai Central Hospital, and Nishidai Clinic, Tokyo, Japan

Several studies have shown that fluorine-18 fluorodeoxyglucose (FDG) positron emission tomography (PET) is not useful for the diagnosis of thymoma. We describe 3 patients with thymoma who underwent both FDG-PET

Accepted for publication Jan 5, 2005.

Address correspondence to Dr Ohtsuka, Department of Thoracic Surgery, Saiseikai Central Hospital, 1-4-17 Mita, Minato-ku, Tokyo, 108-0073 Japan; e-mail: t-oh@remus.dti.ne.jp.

0003-4975/06/$32.00
doi:10.1016/j.athoracsur.2005.01.024

and carbon-11 (11C) acetate (AC)-PET. Although all three thymomas were successfully imaged by AC-PET, one of the thymomas was not imaged by FDG-PET. These results suggest that AC-PET may have a potentially important role in the diagnosis of thymoma. This is the first report of the use of AC-PET for diagnostic imaging of thymoma.

(Ann Thorac Surg 2006;81:1132–4)

Recently, carbon-11 (11C) acetate (AC)-PET has been reported to be of clinical value for the diagnosis of cancers that are not imaged by fluorine-18 fluorodeoxyglucose (FDG)-PET, such as prostate cancer and hepatocellular carcinoma [1, 2]. Here we describe three cases of thymoma that were imaged by AC-PET.

Case Reports

Between June and September 2004, 3 patients with thymomas underwent whole-body FDG-PET and AC-PET. The characteristics of the 3 patients are summarized in Table 1. After obtaining the patients' informed consent, AC-PET was performed before FDG-PET on the same day. The dosage of 11C acetate administered was 125 μCi/kg (4.6 MBq/kg). Positron emission tomographic imaging was performed approximately 10 minutes after administration of AC using a POSICAM.HZL mPOWER (Positron Co, Houston, Texas). The emission scans were initially obtained in two-dimensional mode for 4 minutes per bed position and taken from the top of the skull to the thighs. Approximately 30 minutes after AC-positron emission tomographic imaging, fluorine-18 FDG was administered (ie, more than 120 minutes after administration of the acetate). The dosage of FDG was 125 μCi/kg (4.6 MBq/kg) for nondiabetic patients and 150 μCi/kg (5.6 MBq/kg) for diabetic patients, as we reported previously [3]. The FDG-PET scans were performed approximately 45 minutes after administration of FDG. The images were reconstructed using the emission scans and the preinjection transmission scans in a 128 × 128 matrix by ordered subset expectation maximization corresponding to a pixel size of 4 × 4 mm, with a section spacing of 2.56 mm.

Patient 1

Chest computed tomography (CT) showed a tumor located in the anterior mediastinum, measured 3 × 3 cm (Fig 1A). An AC-positron emission tomographic scan showed accumulation at the tumor site with a standardized uptake value (SUV) of 3.5 (Fig 1B), although FDG-PET showed no accumulation with an SUV of 1.0 (Fig 1C). Thymothymectomy was performed, and histopathologic examination showed a thymoma (World Health Organization [WHO] type AB), which had invaded the capsule.

Patient 2

Chest CT showed a tumor measuring 4 × 4 cm located in the anterior mediastinum (Fig 1D). An 11C-acetate PET showed accumulation at the tumor site with an SUV of 2.7. (Fig 1E), and FDG-PET also showed accumulation at the tumor site with an SUV of 5.9 (Fig 1F). Thymothymectomy was performed and histopathologic examination showed a thymoma (WHO type B1) that had invaded the capsule.

Patient 3

Chest CT showed a tumor located in the anterior mediastinum, measuring 7 × 7 cm (Fig 1G). An AC-PET showed strong accumulation at the tumor site with an SUV of 5.9 (Fig 1H), although FDG-PET showed accumulation with an SUV of 3.1 (Fig 1I). Thymothymectomy was performed, and histopathologic examination showed a thymoma (WHO type AB) that had invaded the capsule.

Comment

Thymic tumors are the most common tumors arising in the anterior mediastinum. Clinically the diagnosis of thymic tumors is performed mainly by morphologic examinations, such as CT and magnetic resonance imaging (MRI). Although both CT and MRI have also been reported to be useful for the differential diagnosis of thymic tumors [4], such diagnosis still remains difficult in some cases. FDG-PET has been reported to show high uptake of FDG in thymic cancer, but not in thymoma [5], probably due to its slow growth [6], and low glucose uptake. In the present report we have described three patients of thymomas that were positively imaged by AC-PET. Acetate has been used as a positron-emitting tracer for measurement of oxidative metabolism in the myocardium. The mechanism by which acetate shows high accumulation in tumor cells is still unknown, although it is considered to differ from that of myocardial uptake [7, 8]. Several studies have shown that 11C acetate has higher sensitivity for the detection of prostate cancer [2] and higher sensitivity and specificity for the diagnosis

Table 1. Characteristics of 3 Thymoma Patients

			Standardized Uptake Value				
	Sex	Age	Acetate Positron Emission Tomography	Fluorodeoxyglucose Positron Emission Tomography	Tumor size (cm)	TNM	Histologic Subtype (World Health Organization)
Patient 1	Male	56	3.5	1.0	3 × 3	T2N0M0	AB
Patient 2	Male	35	2.7	5.9	4 × 4	T2N0M0	B1
Patient 3	Female	65	5.9	3.1	7 × 7	T2N0M0	AB

Ann Thorac Surg
2006;81:1134–6

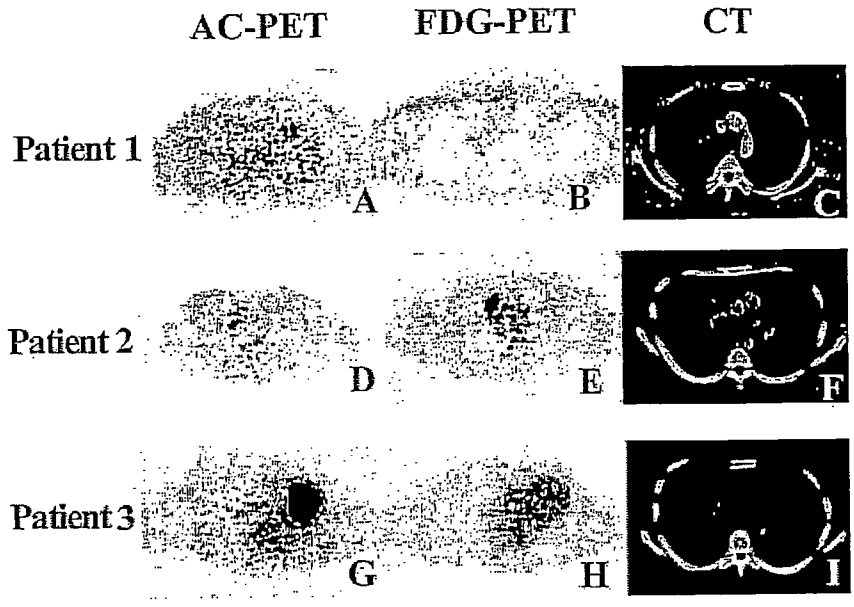

Fig 1. Acetate-positron emission tomography (AC-PET), fluorodeoxyglucose-positron emission tomography (FDG-PET), and computed tomography (CT) in 3 thymoma patients. All 3 thymomas were successfully imaged by AC-PET (A, D, G). By FDG-PET, 2 patients were imaged (E, H), but one was not imaged (B). Chest CT showed anterior mediastinal tumors (C, F, I).

of well-differentiated hepatocellular carcinoma than FDG-PET [1]. Higashi and colleagues [8] described a case of bronchioloalveolar carcinoma in which FDG-PET showed lower uptake than the AC-PET did, suggesting that acetate might accumulate in slow-growing tumors.

We have demonstrated that three patients of thymoma were positively imaged by AC-PET despite showing different results with FDG-PET. Our findings suggest that AC-PET may have a potentially important role in the diagnosis of thymoma, as is the case for other slow-growing tumors such as prostate cancer and bronchioloalveolar carcinoma.

References

1. Ho CL, Yu SC, Yeung DW. 11C-acetate PET imaging in hepatocellular carcinoma and other liver masses. J Nucl Med 2003;44:213–21.
2. Oyama N, Akino H, Kanamaru H, et al. 11C-acetate PET imaging of prostate cancer. J Nucl Med 2002;43:181–6.
3. Nomori H, Watanabe K, Ohtsuka T, Naruke T, Suemasu K, Uno K. Evaluation of F-18 fluorodeoxyglucose (FDG) PET scanning for pulmonary nodules less than 3 cm in diameter, with special reference to the CT images. Lung Cancer 2004; 45:19–27.
4. Molina PL, Siegel MJ, Glazer HS. Thymic masses on MR imaging. AJR Am J Roentgenol 1990;155:495–500.
5. Sasaki M, Kuwabara Y, Ichiya Y, et al. Differential diagnosis of thymic tumors using a combination of 11C-methionine PET and FDG PET. J Nucl Med 1999;40:1595–601.
6. Lewis JE, Wick MR, Scheithauer BW, Bernatz PE, Taylor WF. Thymoma: a clinicopathologic review. Cancer 1987;60:2727–43.
7. Yoshimoto M, Waki A, Yonekura Y, et al. Characterization of acetate metabolism in tumor cells in relation to cell proliferation: acetate metabolism in tumor cells. Nucl Med Biol 2001;28:117–22.
8. Higashi K, Ueda Y, Matsunari I, et al. 11C-acetate PET imaging of lung cancer: comparison with 18F-FDG PET and 99mTc-MIBI SPET. Eur J Nucl Med Mol Imaging 2004;31:13–21.

0003-4975/06/$32.00
doi:10.1016/j.athoracsur.2005.02.093

doi:10.1510/icvts.2006.131722

INTERACTIVE CARDIOVASCULAR AND THORACIC SURGERY

Interactive CardioVascular and Thoracic Surgery 5 (2006) 794-795

www.icvts.org

Case report - Thoracic general

Endoscopic drainage of an infected giant bulla

Iwao Takanami*

Department of Surgery, Teikyo School of Medicine, 2-11 Kaga 2-Chome, Itabashi-Ku, Tokyo 173, Japan

Received 22 February 2006; received in revised form 14 July 2006; accepted 14 July 2006

Abstract

A 42-year-old man was hospitalized because of an infectious giant bulla. The infected giant bulla did not improve by the administration of antibiotics. Some infectious bullae were considered to be difficult to allow for simple cutaneous drainage, so endoscopic drainage was performed to remove the infection. Our experience with endoscopic abscess drainage is excellent in patients in whom conventional therapy fails. We consider the endoscopic drainage an alternative to percutaneous drainage in patients who have an infectious bulla.

Keywords: Infectious giant bulla; Endoscopic drainage; Video-assisted thoracoscope

1. Introduction

The most common therapeutic approach to infectious bullae of the lung is the administration of systemic antibiotics [1]. Surgical resection was reported to be a contraindication in fluid-filled bullae because of persistent postoperative air leakage due to lung injury [1]. If the conservative treatment with antibiotics fails, drainage is usually considered [2]. No report has been published on the endoscopic drainage of an infected bulla. We describe endoscopic drainage of an infected giant bulla and suggest this may present a viable treatment option for cases in which the infection does not resolve with conservative therapy.

2. Case report

A 42-year-old man was admitted to our hospital with complaints of fever. Bullae of the right lung had been found 5 years earlier during a periodic healthy examination. On admission, an examination revealed a male patient in moderate distress with a temperature of 38.5 °C. A chest roentgenogram and CT scans of the chest showed some bullous lesions with niveau-like shadow in the right upper lobe of the lung (Figs. 1 and 2). Sputum and blood cultures were obtained, and therapy was begun with the plan to manage his disease conservatively. An analysis of sputum disclosed no significant findings, and blood culture showed no growth. Laboratory examination revealed that his white blood count was 11700/mm^3, and C-reactive protein was 14.5 mg/dl. The patient continued to have a daily temperature of 39 °C, and white blood count and C-reactive protein were high despite a number of changes in antibiotic therapy. The infected giant bulla did not improve by the administration of antibiotics, and it was concluded that the contents of the bulla needed to be drained. Although thoracostomy tube-drainage for fluid-filled bullae has been described [2], some infectious bullae were considered to be difficult to allow for simple cutaneous drainage. So endoscopic drainage was performed to remove the infection. The patient underwent general anesthesia, and endoscopic surgery in the cavity was performed with the patient in a supine position. A skin incision of approximately 3 cm in size was made and thoracostomy was made to introduce a wound edge protector (Lap-Protector FF0707; Hakko; Tokyo, Japan) through the 2nd intercostal space about 5 cm lateral to the parasternal line, and a video-assisted thoracoscope (EL2-TF410 type 31; Fujinon; Tokyo, Japan) was directly introduced from the wound edge protector into the lumen of the bulla. A yellow-turbid fluid was suctioned and caseous necrosis was resected from the bulla wall with the use of thoracic surgery. There were three abscessed bullae, and the interbullous walls were thin. The interbullous walls were easily opened, and the internal trabeculae were excised by using endoscopic scissors to help drainage more efficiently. An air leakage test showed no air leakage from the inside wall of the bulla. A tube was inserted percutaneously for drainage. Suction at 10 cm water pressure was applied to the tube. Culture of the fluid for routine bacteria, fungal, and tuberculous organisms showed no growth. The infection subsided on the next day, and laboratory examination revealed that white blood count and C-reactive protein soon became within normal range. A subsequent radiograph and CT scan of the chest demonstrated a near-complete resolution of the bullae. The patient was discharged following two weeks of drainage

*Corresponding author. Tel.: +81-3-3317-4057, 81-3-3964-1228; fax: +81-3-3962-2128.

E-mail address: takanami@med.teikyo-u.ac.jp (I. Takanami).

Fig. 1. A chest roentgenogram of a 42-year-old man with air-fluid levels within the giant bullae.

without complications, and he has remained asymptomatic for 6 months.

3. Discussion

We report this case because there have been no previous reports in the literature on the endoscopic drainage of an infected giant bulla. Intracavity suction and drainage was a safe and effective treatment of emphysematous bulla in patients considered to be at poor risk for formal thoracotomy [2]. The percutaneous insertion of a catheter to drain an infectious bulla would be favorable. But if the patient had some infectious bullae, the infection following a catheter insertion may be persistent because a catheter could

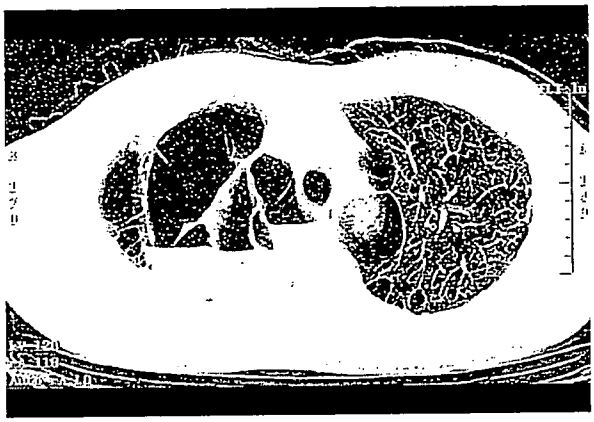

Fig. 2. A chest CT scan showing the presence of some fluid-filled bullae.

not always lead to resolution of all fluid-filled bullae. Thus, the percutaneous drainage may be problematic if anatomic sutures do not allow for access to some of the infectious cavities. Nomori et al. [3] reported that opening of a bulla with the use of video-assisted thoracoscopic surgery (VATS) from the thoracic cavity was effective for infectious bulla. The VATS from the thoracic cavity would be difficult if the lungs firmly adhered to the thoracic wall. Also the risk of empyema following the opening of an infectious bulla may be present. Endoscopic drainage does not carry the risk of soiling the pleural space. Our experience with endoscopic abscess drainage is excellent in patients in whom conventional therapy fails. A subsequent CT scan of the chest demonstrated a near-complete resolution of the bulla. When an infected bulla does not improve by the administration of antibiotics, we think the endoscopic drainage is indicated. We consider the endoscopic drainage an alternative to percutaneous drainage in patients who have infectious bulla.

References

[1] Mahler DA, D'Esopo ND. Periemphysematous lung infection. Clin Chest Med 1981;2:51–57.

[2] Kirschner LS, Stuffer W, Krenzel C, Duane PG. Management of a giant fluid-filled bulla by closed-chest thoracostomy tube drainage. Chest 1997;111:1772–1774.

[3] Nomori H, Horio H, Fuyuno G, Kobayashi R, Morinaga S, Suematsu K. Opening of infectious giant bulla with use of video-assisted thoracoscopic surgery. Chest 1997;112:1670–1673.

Clinico-Pathological and Biological Significance of Tyrosine Kinase Domain Gene Mutations and Overexpression of Epidermal Growth Factor Receptor for Lung Adenocarcinoma

Kouki Ohtsuka, MD, PhD,† Hiroaki Ohnishi, MD, PhD,† Go Furuyashiki, MD,* Hiroshi Nogami, MD, PhD,* Yoshihiko Koshiishi, MD, PhD,* Akiko Ooide, BSc,† Satsuki Matsushima, BSc,† Takashi Watanabe, MD, PhD,† and Tomoyuki Goya, MD, PhD**

Introduction: Mutations in the tyrosine kinase domain (TKD) of the epidermal growth factor receptor (*EGFR*) gene have proven to be clinically significant in non-small cell lung cancer. However, relationships between these mutations and EGFR expression or deletion mutations in the extracellular domain of *EGFR* (*EGFR*vIII) remain unclear. The purpose of this study was to gain further insight into the clinical significance of these molecular abnormalities in lung adenocarcinoma.

Methods: We investigated *EGFR* TKD mutations using direct sequencing, EGFR protein expression using Western blotting, and *EGFR*vIII using reverse transcriptase–polymerase chain reaction in samples from 48 adenocarcinoma patients. Correlations with various clinico-pathological features were analyzed.

Results: *EGFR* TKD mutations were detected in 25 of 48 adenocarcinomas (52.1%), and overexpression of EGFR protein was identified in 19 patients (39.6%). Presence of *EGFR* TKD mutations was significantly correlated with EGFR overexpression ($p = 0.021$). *EGFR* TKD mutations were significantly correlated with never-smoker status ($p = 0.043$), absence of emphysematous or fibrotic appearance on computed tomography ($p = 0.001$), papillary subtype ($p = 0.041$), and bronchioloalveolar carcinoma features ($p = 0.045$). *EGFR*vIII was not detected in any adenocarcinomas. Retrospective analysis revealed that patients with *EGFR* TKD mutations displayed better postoperative prognosis than patients with wild-type *EGFR* ($p = 0.033$).

Conclusions: These results suggest that *EGFR* TKD mutation is associated with EGFR overexpression, representing an important factor for consideration when investigating the clinical significance, including susceptibility to chemotherapy, of *EGFR* TKD mutations in adenocarcinoma. *EGFR*vIII does not seem to play a major role in the development of lung adenocarcinoma.

From the Departments of *Surgery and †Laboratory Medicine, Kyorin University, Tokyo, Japan.

Address for correspondence: Dr. Kouki Ohtsuka, Department of Laboratory Medicine, Kyorin University, 6-20-2, Shinkawa, Mitaka, Tokyo 181-8611, Japan. E-mail: kouki7@kj9.so-net.ne.jp

ISSN: 1556-0864/06/0108-0787

Key Words: Lung cancer, Epidermal growth factor receptor, Mutation, *EGFR*vIII, Overexpression.

(*J Thorac Oncol.* 2006;1: 787–795)

Non-small cell lung cancer (NSCLC) represents one of the major causes of death in developed countries.[1] NSCLC patients often relapse after surgery,[2] and many patients who are treated using conventional cytotoxic agents experience cancer recurrence.[3] New therapeutic modalities are thus required for patients who prove resistant to conventional approaches.

Epidermal growth factor receptor (EGFR) is a member of the receptor-type tyrosine kinase (TK) family, and the molecular status of EGFR in NSCLC has been extensively analyzed. Initially, overexpression of the EGFR protein or gene in NSCLC was frequently reported.[4] Deletion in exons 2 to 7 of the *EGFR* gene (*EGFR*vIII or del2-7*EGFR*), which is often found in glioblastoma or glioma,[5–7] has also been identified in a subset of NSCLC patients.[8–10] Overexpressed EGFR is considered to aberrantly activate downstream signal proteins beyond physiological levels. *EGFR*vIII also has been proven to activate these signal proteins and confer proliferative properties to glioblastoma or glioma cells.[5] Thus, it seems reasonable that EGFR inhibitors might display antitumor activities against cancers harboring EGFR overexpression or *EGFR*vIII. In fact, some studies have confirmed positive correlations between EGFR expression level and efficiency of gefitinib, a major TK inhibitor (TKI) specific for EGFR,[11] although negative results have also been reported.[12]

More recently, small mutations in the TK domain (TKD) of the *EGFR* gene have frequently been found in NSCLC, particularly in adenocarcinomas.[13,14] Interestingly these types of mutations are widely recognized as occurring more frequently in female patients, nonsmokers, tumors with adenocarcinomatous histology, and Asian populations.[15,16] *EGFR* with such mutations as delE746-A750 in exon 19 and L858R in exon 21 is considered to be constitutively activated through phosphorylation, and it displays tumorigenic properties.[13–15,17] Numerous studies have thus reported that

NSCLCs with TKD mutations in the *EGFR* gene tend to show better response to gefitinib than tumors without such mutations.[18,19]

These results suggest that clinical features of NSCLC (and adenocarcinoma in particular), including response to gefitinib, may be associated with both *EGFR* mutations and expression level. Investigation of the correlations between *EGFR* mutations and expression level and exploration of relationships with various clinico-pathological features of adenocarcinoma is therefore meaningful. However, few studies have simultaneously investigated *EGFR* mutations and expression by Western blotting in adenocarcinoma, and no studies investigating *EGFR* TKD mutations have thoroughly analyzed the presence or absence of *EGFR*vIII. Furthermore, previous studies have included only limited information on patient characteristics such as sex and smoking status.[15] The present study investigated *EGFR* mutations, both in terms of *EGFR* TKD mutations and *EGFR*vIII, and concurrently examined expression levels of EGFR in clinical lung adenocarcinoma samples. The results were then correlated with various clinico-pathological features.

MATERIALS AND METHODS

Patients

A total of 96 Japanese patients with NSCLC underwent surgery in the Department of Thoracic Surgery at Kyorin University Hospital between May 2001 and March 2003. Of these, 48 patients with adenocarcinoma diagnosed by a trained pathologist were enrolled for further analysis. All patients underwent pulmonary resection with or without lymph node dissection. After surgery, some patients underwent chemotherapy and/or radiotherapy with various regimens. No patient was administered gefitinib before tumor recurrence. Written informed consent to analyze tissue DNA, RNA, and protein was obtained from each patient prior to operation. The authors who conducted molecular analyses were blinded to the postoperative outcomes of all patients until all molecular analyses were completed.

Patient Data

Various clinical data were obtained from in- and outpatient medical records. Clinical and pathological stages of adenocarcinoma patients were determined in accordance with the criteria of the tumor-node metastasis classification system.[20] The following criteria were used to classify smoking status: never smoker, patients who had smoked fewer than 100 cigarettes in their lifetime; former smoker, patients who had stopped smoking at least 12 months before diagnosis; and current smoker. Percentage of forced expiratory volume in 1 second was measured preoperatively in all patients and used as a parameter for respiratory function. Levels of carcinoembryonic antigen were determined in all patients at the time of diagnosis as a serological tumor marker. Computed tomography (CT) was performed and interpreted by radiologists in the Department of Radiology at Kyorin University Hospital who were blinded to EGFR status. Presence of ground-glass opacity components within the tumor region and emphysematous or fibrotic appearance in adjacent lung tissue was integrated into the analysis. The World Health Organization classification system also was used for pathological subclassification of adenocarcinomas regarding papillary subtype and level of differentiation.[21] Status of bronchioloalveolar carcinoma (BAC) features was determined using a report from the Memorial Sloan-Kettering Cancer Center.[22] Responses to conventional cytotoxic agents or gefitinib were assessed using the response evaluation criteria in solid tumors.[23]

Samples

Lung cancer cell lines NCI-H1650 and H1975 were purchased from American Type Culture Collection (Manassas, VA) and used as positive controls for mutations.[17] Glioblastoma cell line U87MGΔ*EGFR* with *EGFR*vIII was kindly donated by Professor Webster K. Cavenee of the Ludwig Institute for Cancer Research in San Diego and was used as a positive control for *EGFR*vIII mutation.[24] Tumor samples and visually normal lung tissues distant from the tumor were immediately frozen after resection and preserved at −80°C. Visually normal lung tissues were confirmed as containing no tumor component on pathological examination.

Direct Sequencing

Mutations of *EGFR* in lung cancer tend to cluster within exons 18 to 21. Direct sequencing analysis of *EGFR* from exons 18 to 21 was therefore performed using previously reported methods[25] for all samples, including the two positive-control NSCLC cell lines.

Reverse Transcriptase–Polymerase Chain Reaction

*EGFR*vIII is generated by total (801 bp) deletion of exons 2 to 7 in the extracellular domain of the *EGFR* gene. Because reverse transcriptase–polymerase chain reaction (RT-PCR) is reportedly useful in detecting this deletion in glioblastoma,[5] it was employed in this study. For detection of the 801-bp deletion, tumor cDNA and primers (Table 1) were subjected to 40 cycles of polymerase chain-reaction amplification.

Western Blotting

For EGFR Western blotting analysis, 100 μg of tumor or normal-lung protein was used. Samples were subjected to Western blotting analyses using anti-EGFR monoclonal antibody (BD Biosciences, San Jose, CA) according to the instructions of the manufacturer. This antibody binds to the intracellular domain of EGFR protein (amino acids 1020–1046) distant from TKD. Equal loading of extract was confirmed by Western blotting using anti-β-actin antibody (Sigma, St. Louis, MO). Normal-lung protein usually demonstrated either a very weak EGFR band (180 kDa) or no band on Western blotting. The EGFR expression level for each tumor was determined in comparison with expression in corresponding normal-lung protein as follows: (−), very weak or no band similar to normal lung; (+), easily visible band; and (2+), very strong band similar to levels of cell lines. An EGFR expression level of (+) or (2+) was defined as indicating EGFR overexpression.

TABLE 1. *EGFR* Primers

	Nucleotide
PCR primers	
Exon 18 sense	5′-CAAGTGCCGTGTCCTGGCACCCAAGC-3′
Exon 18 antisense	5′-CCAAACACTCAGTGAAACAACAAA GAG-3′
Exon 19 sense	5′-TGCATCGCTGGTAACAT-3′
Exon 19 antisense	5′-AGCTGCCAGACATGAGAA-3′
Exon 20 sense	5′-ATTCATGCGTCTTCACCTGG-3′
Exon 20 antisense	5′-TGAGAGTTTCCACATGCAGAT-3′
Exon 21 sense	5′-TGGTCAGCAGCGGGTTACATCTTC-3′
Exon 21 antisense	5′-CAATACAGCTAGTGGGAAGGCAGC-3′
Sequencing reaction primers	
Exon 18 sense	5′-CTTTCCAGCATGGTGA-3′
Exon 18 antisense	5′-GATGGAAATATACAGC-3′
Exon 19 sense	5′-ACCATCTCACAATTGCCAG-3′
Exon 19 antisense	5′-TGAGGTTCAGAGCCAT-3′
Exon 20 sense	5′-AGGAAGCCTACGTGAT-3′
Exon 20 antisense	5′-TGAGAGTTTCCACATGCAGAT-3′
Exon 21 sense	5′-CTTTGGATCAGTAGTC-3′
Exon 21 antisense	5′-CTGGCTGACCTAAAGC-3′
Exons 2-7 RT-PCR primers	
Exons 2-7 RT-PCR sense	5′-GTATTGATCGGGAGAGCCG-3′
Exons 2-7 RT-PCR antisense	5′-GTGGAGATCGCCACTGATG-3′

Statistical Analysis

The significance of differences in categorical data was tested using the χ^2 test or Fisher's exact test. Logistic regression analysis was performed to determine independent corresponding factors. Differences in overall survival and time to progression (TTP) after surgery according to presence or absence of *EGFR* gene mutations or EGFR protein overexpression were compared using Kaplan-Meier curves and log-rank tests. SPSS for Windows version 11.0 software (SPSS, Chicago, IL) was used to perform all statistical calculations. All statistical tests were two sided, and differences were considered statistically significant for values of $p < 0.05$.

RESULTS

Patient Characteristics

Patients comprised 21 women (43.8%) and 27 men (56.3%). Median age for the 48 patients was 68.5 years (range, 42–83 years). Subjects comprised 24 never smokers (50.0%), 17 former smokers (35.4%), and seven current smokers (14.6%). Clinical stages of patients were as follows: stage IA (T1 N0 M0) in 22 patients (45.8%); stage IB (T2 N0 M0) in 16 patients (33.3%); stage IIA (T1 N1 M0) in one patient (2.1%); stage IIB (T2 N1 M0 or T3 N0 M0) in two patients (4.2%); stage IIIA (T1–3 N2 M0 or T3 N1–2 M0) in six patients (12.5%); and stage IIIB (T4 any N M0 or any T N3 M0) in one patient (2.1%). Pathological stages were as follows: stage IA in 14 patients (29.2%); stage IB in 11 patients (22.9%); stage IIA in three patients (6.25%); stage IIB in four patients (8.3%); stage IIIA in six patients (12.5%); stage IIIB in seven patients (14.6%); and stage IV (any T any N M1) in three patients (6.25%). Details of other characteristics are shown in Tables 2 and 3.

Mutations and Expression of EGFR in Cell Lines

Direct sequencing analysis was performed for NCI-H1650 and H1975, confirming that both cell lines possess the expected mutations (H1650: deletion of nt.2481-2495; H1975: L858R and T790M). Western blotting demonstrated very strong EGFR expression levels in both cell lines, suggesting overexpression of EGFR. H1975 displayed another band of approximately 50 kDa (Figure 1A).

EGFR TKD Mutations in Patient Samples

EGFR mutations in TKD are summarized in Table 2. At least one of of the mutations within exons 18 to 21 was found in 25 of the 48 adenocarcinomas (52.1%).

Deletions in exon 19 were found in 11 of 48 adenocarcinoma samples (22.9%). Types of deletion varied, but eight of the 11 mutations were delE746-A750 (i.e., either Del1 [del nt.2481-2495] or Del2 [del nt.2482-2496]). Each of the remaining three patients displayed a different type of mutation: Del3 (delL747-T751), Del4 (delE746-R748), and Del5 (delL747-P753insS).

Mutations within exon 21 were found in 13 of 48 adenocarcinomas (27.1%), and all were identical to the L858R mutation. Two adenocarcinoma patients with L858R displayed a second mutation, one with E709G in exon 18, and the other with H870R in exon 21.

Mutation within exon 18 was found in only one patient (2.1%). This mutation was the previously reported E709G, and the patient also displayed L858R. Another patient exhibited a 1-bp insertion at intron 17, but sequencing analysis of cDNA revealed that cDNA of the sample from this patient was wild type, indicating that the insertion did not affect mRNA formation. This mutation was considered a silent mutation and was not included for further analysis.

Mutation within exon 20 was found in only one patient (2.1%). This patient displayed an N771SinsH mutation in exon 20 that had not previously been reported in NSCLC (Figure 2A).

*EGFR*vIII in Patient Samples

We performed RT-PCR of the *EGFR* extracellular domain in 48 adenocarcinoma samples, but none showed a short 352-bp band. These results indicate that no adenocarcinoma samples in this study contained *EGFR*vIII mutations (Table 2, Figure 2B).

EGFR Protein Expression in Patient Samples

Expression levels of EGFR protein were categorized into three groups using Western blotting analysis: (2+), (+), and (−). Because all normal-lung samples showed (−) (weak or negative) EGFR expression in our study, tumor samples with (2+) or (+) expression were considered representative of EGFR overexpression. Expression levels of β-actin were (2+) in all tumor and normal-lung samples, suggesting that the protein samples were suitable for analysis (Figure 1B). EGFR overexpression was present in 19 of the 48 patients

TABLE 2. Characteristics of Adenocarcinoma Patients

Case	Age (yr)	Sex	Smoking	Pathological stage	Histologic subtype	BAC features	Differentiation	*EGFR* mutations	EGFR expression	Recurrence	Gefitinib response
1	80	F	N	IB	Pap	AD	Mod	Del2 (exon 19)	−	Yes	
2	42	M	F14	IIIB	Pap	AD	Well	Del1 (exon 19)	2+		
3	63	M	C41	IIA	Others	AWBF	Mod	Del2 (exon 19)	+	Yes	
4	56	M	F5	IV	Others	AD	Well	Del1 (exon 19)	2+	Yes	PR
5	57	F	N	IB	Pap	AWBF	Well	Del1 (exon 19)	+		
6	66	F	N	IA	Others	AWBF	Well	Del3 (exon 19)	+		
7	60	M	F44	IB	Pap	AD	Well	Del4 (exon 19)	+		
8	68	F	N	IIA	Pap	AWBF	Mod	Del2 (exon 19)	−		
9	76	M	N	IA	Pap	AWBF	Well	Del5 (exon19)	+		
10	54	F	N	IIIA	Pap	AWBF	Well	Del1 (exon 19)	−		
11	70	M	F13	IV	Others	AD	Poor	Del1 (exon 19)	2+		
12	79	F	N	IA	Pap	AWBF	Well	N771S insH (exon 20)	−		
13	70	F	N	IB	Others	AWBF	Well	L858R (exon 21) and H870R (exon 21)	2+		
14	64	F	N	IA	Pap	AWBF	Mod	L858R (exon 21)	+		
15	70	F	N	IA	Pap	AD	Mod	L858R (exon 21)	+		
16	54	F	N	IIIB	Pap	AWBF	Poor	L858R (exon 21)	−	Yes	SD
17	62	F	N	IIIA	Pap	AWBF	Mod	L858R (exon 21)	+	Yes	
18	56	M	N	IIIB	Pap	AWBF	Well	L858R (exon 21)	−	Yes	SD
19	65	F	N	IIIA	Pap	AWBF	Mod	L858R (exon 21)	+	Yes	
20	70	F	F30	IIA	Pap	AD	Well	L858R (exon 21)	−		
21	77	M	C29	IIIB	Pap	AWBF	Well	L858R (exon 21)	−	Yes	
22	81	M	N	IV	Pap	AWBF	Mod	L858R (exon 21)	−	Yes	
23	76	M	F56	IA	Pap	AWBF	Well	L858R (exon 21)	−		
24	60	F	N	IA	Pap	AWBF	Well	L858R (exon 21) and E709G (exon18)	+	Yes	
25	69	M	F25	IA	Pap	AWBF	Mod	L858R (exon 21)	−	Yes	
26	73	F	N	IIIB	Pap	AD	Mod	WT (Intron 17 ins)	+	Yes	PD
27	69	M	C26	IA	Others	AD	Well	WT	−		
28	66	M	F80	IB	Others	AWBF	Well	WT	−	Yes	
29	59	M	F35	IIB	Others	AD	Poor	WT	2+	Yes	
30	73	M	F75	IIIA	Pap	AWBF	Well	WT	−	Yes	SD
31	81	M	F88	IA	Pap	AWBF	Well	WT	−	Yes	PD
32	61	F	F22	IB	Others	AD	Poor	WT	−		
33	70	M	F10	IB	Pap	AWBF	Well	WT	−		
34	56	F	N	IIIB	Others	AWBF	Well	WT	−		
35	78	M	F200	IIB	Pap	AD	Mod	WT	+		
36	81	M	N	IB	Others	AWBF	Poor	WT	−	Yes	
37	74	M	F60	IA	Others	AWBF	Poor	WT	−	Yes	
38	52	F	N	IA	Pap	AWBF	Well	WT	−		
39	69	M	N	IIB	Others	AD	Well	WT	−	Yes	PD
40	50	F	N	IIIA	Others	AD	Poor	WT	+	Yes	PD
41	68	M	C30	IA	Pap	AD	Mod	WT	−		
42	54	M	F20	IA	Others	AD	Mod	WT	−	Yes	
43	75	M	F60	IB	Others	AD	Poor	WT	−		
44	83	F	N	IB	Pap	AWBF	Well	WT	−	Yes	
45	75	F	N	IIIB	Pap	AWBF	Mod	WT	−	Yes	PD
46	56	M	C64	IIIA	Pap	AD	Mod	WT	+	Yes	
47	50	M	C60	IB	Pap	AD	Mod	WT	−		
48	73	M	C55	IIIB	Pap	AD	Mod	WT	−	Yes	

M, male; F, female; C, current smoker; F, former smoker; N, never smoker; Pap, papillary; BAC, bronchioloalveolar carcinoma; AD, adenocarcinoma without BAC features; AWBF, adenocarcinoma with BAC features; well, well differentiated; mod, moderately differentiated; poor, poorly differentiated; del, deletion mutation; WT, wild type; ins, insertion mutation; Del1, del nt.2481-2495; Del2, del nt.2482-2496; Del3, delL747-T751; Del4, delE746-R748; Del5, delL747-P753insS; PR, partial response; SD, stable disease; PD, progressive disease; NE, not evaluated. Numbers in Smoking column indicate pack-years. "Others" in Histologic subtype column indicates acinar, solid, or BAC.

TABLE 3. Relationship Between *EGFR* TKD Mutations and Clinico-pathological/Molecular Features of Adenocarcinoma Patients

	Total	Mutation	(%)	Wild	(%)	*p* value
n	48	25	52.1	23	47.9	
Sex						
Women	21	14	66.7	7	33.3	
Men	27	11	40.7	16	59.3	0.074
Age (yr)						
<65	19	11	57.9	8	42.1	
≥65	29	14	48.3	15	51.7	0.514
Smoking status						
Never	24	16	66.7	8	33.3	
Current/former	24	9	37.5	15	62.5	0.043[a]
GGO component						
Present	11	6	54.5	5	45.5	
Absent	37	19	51.4	18	48.6	0.382
Emphysematous and/or fibrotic appearance on CT						
Present	8	0	0.0	8	100.0	
Absent	40	25	62.5	15	37.5	0.001[a]
$FEV_{1.0}$%						
≥70	36	20	55.6	16	44.4	
<70	12	5	41.7	7	58.3	0.404
CEA (ng/ml)						
<5	26	16	61.5	10	38.5	
≥5	22	9	40.9	13	59.1	0.154
Differentiation						
Well/mod	40	23	57.5	17	42.5	
Poor	8	2	25.0	6	75.0	0.093
Papillary subtype						
Yes	32	20	62.5	12	37.5	
No	16	5	31.3	11	68.8	0.041[a]
BAC features						
Present	28	18	64.3	10	35.7	
Absent	20	7	35.0	13	65.0	0.045[a]
EGFR expression						
(2+)/(+)	19	14	73.7	5	26.3	
(−)	29	11	37.9	18	62.1	0.015[a]
Pathological stage						
I/II	32	16	50.0	16	50.0	
III/IV	16	9	56.3	7	43.8	0.683
Postoperative recurrence						
Yes	25	11	44.0	14	56.0	
No	23	14	60.9	9	39.1	0.243

GGO, ground-glass opacity; CT, computed tomography; $FEV_{1.0}$% forced expiratory volume in 1 second (%); CEA, carcinoembryonic antigen; BAC, bronchioloalveolar carcinoma. [a] Statistically significant ($p < 0.05$).

(39.5%), with five patients (10.4%) showing (2+) expression. Of the 19 samples with EGFR overexpression, 14 (73.7%) showed *EGFR* TKD mutations (Table 2). In contrast, 11 of 29 (37.9%) samples without overexpression displayed *EGFR* TKD mutations.

Correlation of *EGFR* TKD Mutations with Clinico-Pathological and Molecular Features

Correlations between *EGFR* TKD mutations and various clinical, pathological, and molecular features were investigated in patients with adenocarcinoma (Table 3). Using univariate analysis, never-smoker status ($p = 0.043$), papillary subtype ($p = 0.041$), presence of BAC features ($p = 0.045$), absence of emphysematous or fibrotic appearances on CT ($p = 0.001$), and EGFR overexpression ($p = 0.015$) were found to be significantly correlated with *EGFR* TKD mutations. Under multivariate analysis, EGFR overexpression was the only factor identified as significant ($p = 0.021$).

Gefitinib Response of Patients

A total of nine patients with or without prior chemotherapy were treated using gefitinib after relapse. Response

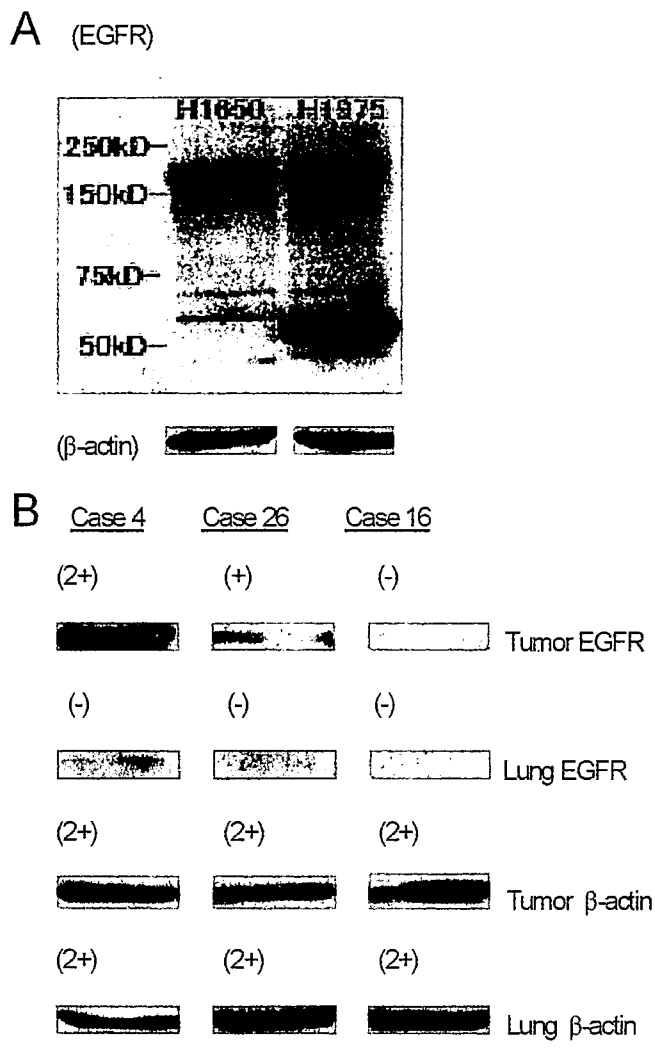

FIGURE 1. EGFR protein expression analysis by Western blotting. EGFR protein expression was classified into three levels: (2+), (+), and (−). (*A*) NCI-H1650 and H1975 cell lines. Both cell lines show strong EGFR expression. (*B*) Clinical samples with (2+) (case 4), (+) (case 26), and (−) (case 16) expression level. EGFR expression of corresponding normal-lung tissue and β-actin expression of tumor and normal-lung tissue are also shown.

rate was 33.3% (one in three) for patients with *EGFR* TKD mutations and 0% (out of six) for patients with wild-type *EGFR*. The sole patient who responded to gefitinib therapy showed both EGFR TKD mutation and EGFR (2+) expression (Table 2).

Survival and TTP in Adenocarcinoma Patients

Figure 3A shows overall survival after surgery in adenocarcinoma patients with or without *EGFR* TKD mutations, according to Kaplan-Meier analysis. The median period of observation was 31.9 months (range, 1.32–48.1 months). Log-rank testing revealed a significant difference in overall survival between patients with mutation-type *EGFR* and those with wild-type *EGFR* ($p = 0.033$). We then analyzed whether the presence or absence of *EGFR* TKD mutation has any influence on the overall survival of patients receiving gefitinib therapy. Among patients treated with gefitinib, those with mutation showed a significantly better overall survival rate than those without mutation. Among patients without gefitinib therapy, however, no differences in overall survival rate were seen between patients with or without mutation (Figure 3B).

Figure 3C shows TTP after surgery for adenocarcinoma patients with or without *EGFR* TKD mutations. Differences in TTP between these two populations were not significant ($p = 0.105$).

Correlations between EGFR expression levels and overall survival were also analyzed (Figure 3D), but no significant difference was identified ($p = 0.385$).

DISCUSSION

This study analyzed correlations between *EGFR* TKD gene mutations in clinical lung adenocarcinoma samples and various clinical, pathological, and molecular features. Most strikingly, the present study offers the first demonstration of correlations between *EGFR* TKD mutations and EGFR overexpression by Western blotting in adenocarcinoma patients. EGFR expression levels were analyzed in all adenocarcinoma samples using Western blotting analysis, revealing that *EGFR* TKD mutations were strongly correlated with EGFR overexpression by Western blotting. *EGFR* TKD mutations were present in 14 of 19 samples with EGFR overexpression (73.7%). This correlation resembles overexpression of the *EGFR* gene in *EGFR*vIII in glioblastoma or glioma, where tumors with *EGFR*vIII are frequently associated with EGFR overexpression through gene amplification. Deletion of the extracellular domain is considered to result from instability caused by gene amplification.[5–7] Along a similar line, tumors with overexpression of the *EGFR* gene may be generated by amplification in lung adenocarcinoma, and *EGFR* TKD mutations may be caused by instability in the amplified gene.[26]

Previously, most studies analyzing EGFR overexpression in lung cancer have used immunohistochemistry (IHC). This method offers the advantage that, under ideal conditions, distributions and proportions of EGFR-positive cells in the tumor can be examined at the cellular level. However, the quality of staining depends largely on the condition of samples and the techniques used, and accurately assessing the proportion of positive cells in tumor is often difficult. In addition, cutoff levels of overexpression can vary considerably among reports, and the rate of EGFR overexpression actually ranges from 20 to 80% in reported cases.[4] These results suggest that IHC is not a very accurate or objective method for evaluating EGFR overexpression. Western blotting, used here for the analysis of EGFR overexpression, allows easy comparison of protein expression levels between tumor and normal-lung samples and is thus assumed to be at least as reliable as IHC.

We also investigated *EGFR*vIII in all samples using RT-PCR, and we found that this mutation was very rare in NSCLC, particularly in adenocarcinomas. Contrary to our findings, two previous studies have reported the presence of *EGFR*vIII in 16 and 39% of NSCLCs, including adenocarci-

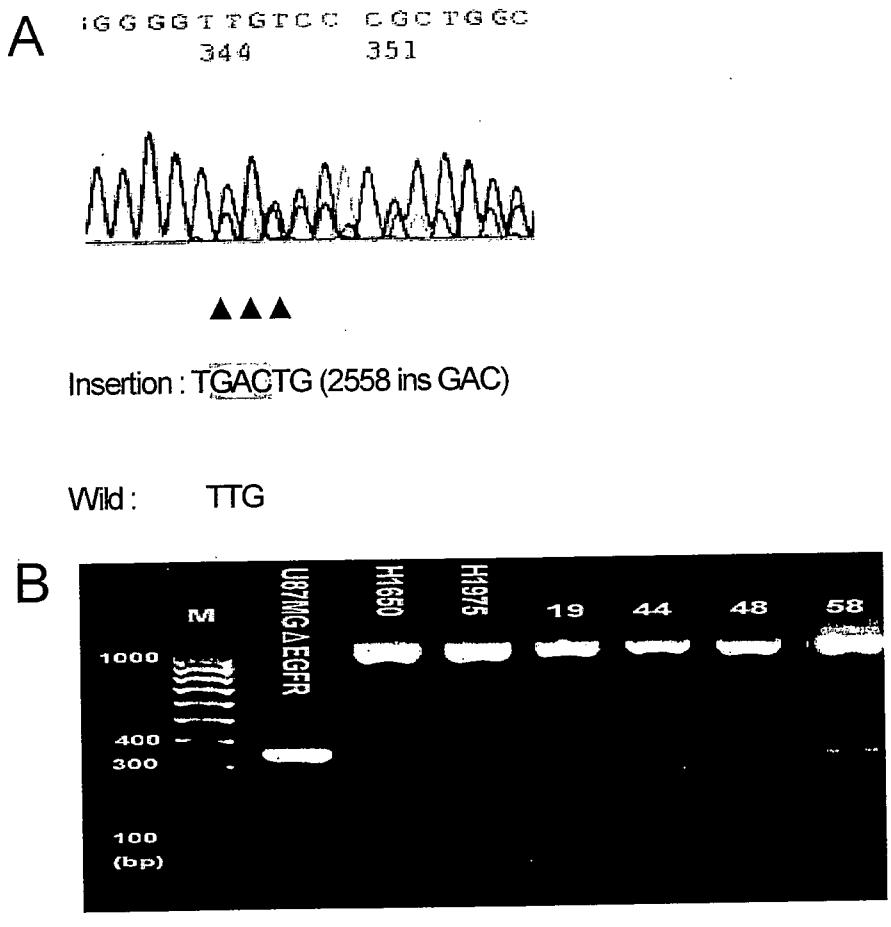

FIGURE 2. *EGFR* mutations. (*A*) N771SinsH in exon 20 (antisense direction); (*B*) results of RT-PCR for detecting *EGFR*vIII. U87MGΔ*EGFR* glioblastoma cell line showed a short 352-bp band, indicating that *EGFR*vIII was included. No adenocarcinoma samples showed a short 352-bp band (cases 19, 44, and 48), but one large-cell carcinoma sample (case 58) showed a weak 352-bp band (not included in the current study).

nomas.[8–10] The reason for this discrepancy is unclear, but differences in methods of detecting *EGFR*vIII may have contributed. RT-PCR as used in our study has been proven to be capable of detecting *EGFR*vIII as efficiently as IHC in glioblastoma.[5] In contrast, the specificity of the antibody used to detect *EGFR*vIII by IHC might have contributed to overestimation of *EGFR*vIII-positive lung cancers in previous studies. Another possible explanation is that *EGFR*vIII could be generated not through the generation of mRNA with deletion of exons 2 to 7, but by alternative mechanisms. Most recently, consistent with our results, a study with a larger number of patients reported that *EGFR*vIII was found only in squamous cell carcinomas, not in adenocarcinomas.[27]

The present study also clarified the correlation of *EGFR* TKD mutations with various clinico-pathological features. Nonsmoker status, papillary subtype, and presence of BAC features were correlated with a high rate of *EGFR* TKD mutations, as already reported in previous studies.[15,19] Among the clinico-pathological factors analyzed, we discovered that an absence of emphysematous or fibrotic appearance on CT was significantly correlated with *EGFR* TKD mutations ($p = 0.001$). In fact, no mutations were found in patients with these findings on CT. This result is interesting because emphysematous or fibrotic appearance on CT is probably a consequence of smoking. Patients with lung cancer often do not objectively declare smoking history, and smoking status by patient declaration does not always reflect the patient's true history of smoking. Emphysematous or fibrotic appearance on CT may have reflected smoking habit more accurately than self-declaration and, accordingly, correlated with absence of *EGFR* TKD mutations. The emphysematous and fibrotic lung itself may also display an association with the development of lung cancer via mechanisms other than *EGFR* TKD mutations.

Although several features have been proven to be associated with *EGFR* TKD mutations, multivariate analysis revealed EGFR overexpression as the sole independent factor correlated with *EGFR* TKD mutations. This result may indicate that EGFR overexpression should be analyzed simultaneously in clinical samples to clarify the clinical significance of *EGFR* TKD mutations.

Prognosis for adenocarcinoma patients after surgery, including gefitinib-treated patients, was also analyzed in relation to *EGFR* TKD mutations. In the present study, overall survival was significantly better in patients with *EGFR* TKD mutations than in patients without such mutations.[16,28] One possible explanation for this finding is that lung adenocarcinomas with *EGFR* TKD mutations are intrinsically more benign than those without these mutations. Alternately, tumors with *EGFR* TKD mutations may be more susceptible to specific therapies, including gefitinib, resulting in better prognosis than tumors without mutations. Although

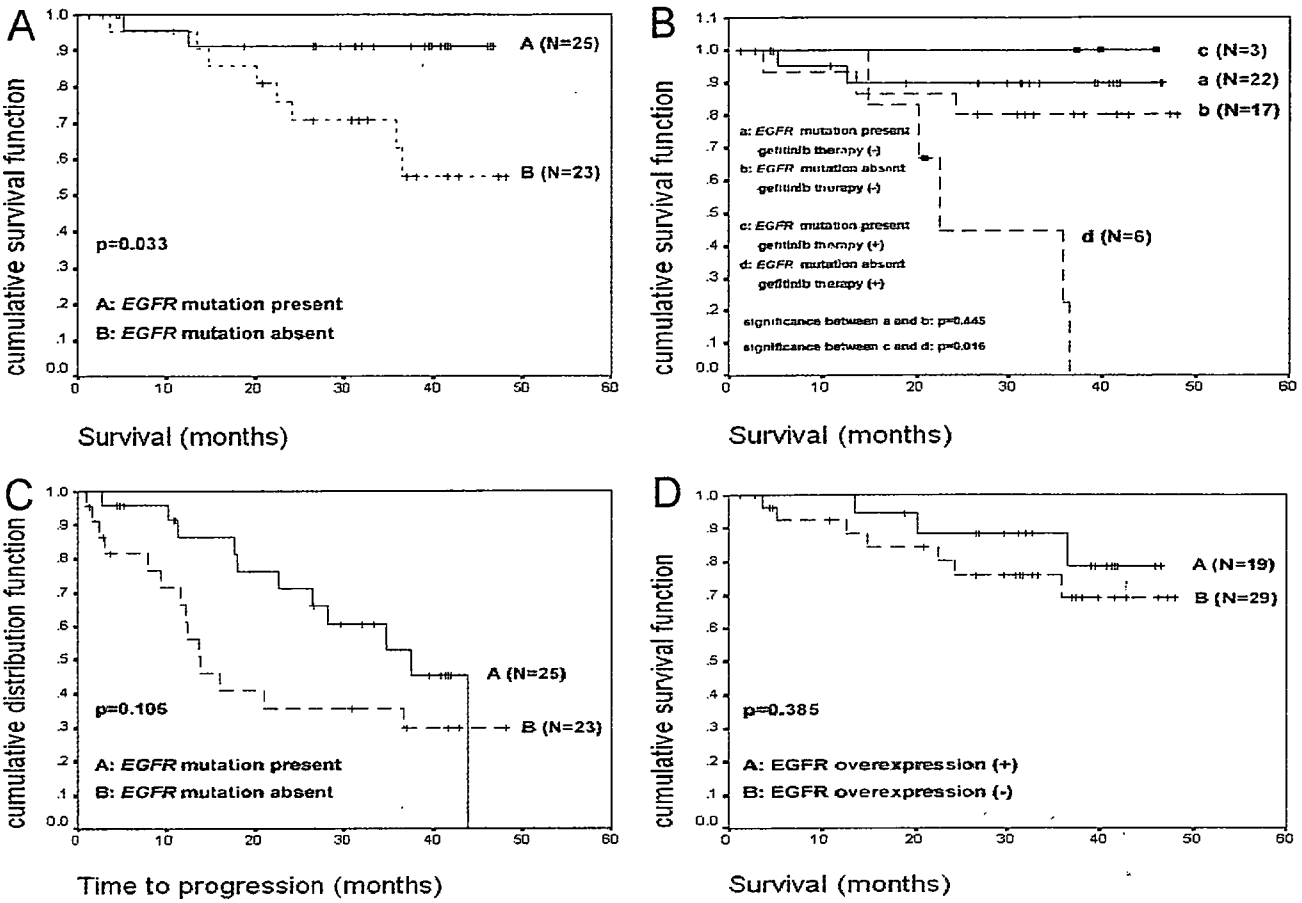

FIGURE 3. Kaplan-Meier analysis of adenocarcinoma patients. (*A*) Overall survival rate after surgery in patients with or without *EGFR* TKD mutations. Log-rank testing revealed that the overall survival rate was significantly better for patients with *EGFR* TKD mutations than for those without mutations ($p = 0.033$). (*B*) The overall rate of survival after surgery was analyzed for gefitinib therapy and *EGFR* mutations. For gefitinib-treated patients, differences between patients with and without *EGFR* mutations were significant ($p = 0.016$). For patients without gefitinib therapy, however, no significant differences were noted between patients with and without *EGFR* mutations ($p = 0.445$). (*C*) TTP after surgery for patients with or without *EGFR* TKD mutations. Differences in TTP between the two populations were not significant ($p = 0.105$). (*D*) Overall survival after surgery for patients with or without EGFR overexpression. Differences were not significant ($p = 0.385$).

the number of patients was small, we have shown in this retrospective study that gefitinib therapy is specifically effective for patients with *EGFR* TKD mutation (Figure 3B). These results may suggest that the latter possibility is more likely. However, further studies based on appropriate study designs, such as randomized control studies, are essential to evaluate the influence of *EGFR* TKD mutations on patient prognosis.

Many previous studies have reported close correlations between susceptibility to gefitinib and various EGFR abnormalities. It has not yet been elucidated whether EGFR abnormalities such as gene amplification, mutation, or EGFR protein overexpression represent the main contributions to response to TKIs. Cappuzzo et al.[29] recently analyzed the effects of *EGFR* gene amplification and TKD mutation on response to gefitinib and showed a stronger correlation for amplification than for TKD mutation. *EGFR* gene copy number (i.e., gene amplification) is also reportedly correlated with EGFR protein overexpression.[30] These results suggest that EGFR protein overexpression is more strongly correlated with response to TKIs than mutation. However, in the present study, using Western blot, EGFR protein overexpression was not directly correlated to gefitinib response (data not shown). This may be attributable to the limited number of patients treated with gefitinib and the retrospective nature of the present study. EGFR protein expression level was analyzed rather than gene amplification in this study because protein expression levels are considered to more directly reflect the amount of EGFR protein to be inhibited by TKIs. We are currently investigating correlations between *EGFR* gene amplification in DNA level and mRNA expression level, and the results of this pending investigation are expected to provide some insight into this issue. The molecular mechanisms underlying gefitinib susceptibility in terms of EGFR expression level and the presence of *EGFR* TKD mutations remain to be determined in future studies.

In conclusion, we have confirmed that EGFR overexpression is closely related to *EGFR* TKD mutations. Analysis

of *EGFR* mutations together with EGFR protein expression level in clinical studies will facilitate an understanding of the role of EGFR in lung cancer and lead to the development of new anticancer agents.

ACKNOWLEDGMENTS

We wish to thank Professor Webster K. Cavenee of the Ludwig Institute for Cancer Research at San Diego for the kind gift of glioblastoma cell line U87MGΔEGFR and Motoo Nagane, MD, PhD from the Department of Neurosurgery at Kyorin University Hospital for his technical advice.

REFERENCES

1. Jemal A, Tiwari RC, Murray T, et al. American Cancer Society. Cancer statistics, 2004. *CA Cancer J Clin* 2004;54:8–29.
2. Goya T, Asamura H, Yoshimura H, et al. Prognosis of 6644 resected non-small cell lung cancers in Japan: a Japanese lung cancer registry study. *Lung Cancer* 2006;50:227–234.
3. Schiller JH, Harrington D, Belani CP, et al. Eastern Cooperative Oncology Group. Comparison of four chemotherapy regimens for advanced non-small-cell lung cancer. *N Engl J Med* 2002;346:92–98.
4. Nakamura H, Kawasaki N, Taguchi M, et al. Survival impact of epidermal growth factor receptor overexpression in patients with non-small-cell lung cancer: a meta-analysis. *Thorax* 2006;61:140–145.
5. Worm K, Dabbagh P, Schwechheimer K. Reverse transcriptase polymerase chain reaction as a reliable method to detect epidermal growth factor receptor exon 2-7 gene deletion in human glioblastomas. *Hum Pathol* 1999;30:222–226.
6. Ekstrand AJ, Sugawa N, James CD, et al. Amplified and rearranged epidermal growth factor receptor genes in human glioblastomas reveal deletions of sequences encoding portions of the N- and /or C-terminal tails. *Proc Natl Acad Sci U S A* 1992;89:4309–4313.
7. Wong AJ, Ruppert JM, Bigner SH, et al. Structual alterations of the epidermal growth factor receptor gene in human gliomas. *Proc Natl Acad Sci U S A* 1992;89:2965–2969.
8. Garcia de Palazzo IE, Adams GP, Sundareshan P, et al. Expression of mutated epidermal growth factor receptor by non-small cell lung carcinomas. *Cancer Res* 1993;53:3217–3220.
9. Okamoto I, Kenyon LC, Emlet DR, et al. Expression of constitutively activated EGFRvIII in non-small cell lung cancer. *Cancer Sci* 2003;94: 50–56.
10. Krause DS, Van Etten RA. Tyrosine kinases as targets for cancer therapy. *N Engl J Med* 2006;353:172–187.
11. Santoro A, Cavina R, Latteri F, et al. Activity of a specific inhibitor, gefitinib (Iresa™, ZD1839), of epidermal growth factor receptor in refractory non-small-cell lung cancer. *Ann Oncol* 2004;15:33–37.
12. Kim KS, Jeong JY, Kim YC, et al. Predictors of the response to gefitinib in refractory non-small cell lung cancer. *Clin Cancer Res* 2006;11:2244–2251.
13. Lynch TJ, Bell DW, Sordella R, et al. Activating mutations in the epidermal growth factor receptor underlying responsiveness of non-small-cell lung cancer to gefitinib. *N Engl J Med* 2004;350:2129–2139.
14. Paez JG, Janne PA, Lee JC, et al. EGFR mutations in lung cancer: correlation with clinical response to gefitinib therapy. *Science* 2004;304: 1497–1500.
15. Pao W, Miller V, Zakowski M, et al. EGF receptor gene mutations are common in lung cancers from "never smokers" and are associated with sensitivity of tumors to gefitinib and erlotinib. *Proc Natl Acad Sci U S A* 2004;101:13306–13311.
16. Shigematsu H, Lin L, Takahashi T, et al. Clinical and biological features associated with epidermal growth factor receptor gene mutations in lung cancers. *J Natl Cancer Inst* 2006;97:339–346.
17. Sordella R, Bell DW, Haber DA, et al. Gefitinib-sensitizing EGFR mutations in lung cancer activate anti-apoptotic pathways. *Science* 2004;305:1163–1167.
18. Mitsudomi T, Kosaka T, Endoh H, et al. Mutations of the epidermal growth factor receptor gene predict prolonged survival after gefitinib treatment in patients with non-small-cell lung cancer with postoperative recurrence. *J Clin Oncol* 2006;23:2513–2520.
19. Takano T, Ohe Y, Sakamoto H, et al. Epidermal growth factor receptor gene mutations and increased copy numbers predict gefitinib sensitivity in patients with recurrent non-small-cell lung cancer. *J Clin Oncol* 2006;23:6829–6837.
20. International Union Against Cancer. Lung Tumors. In Sobin LH, Wittekind CH (Eds.), TNM Classification of Malignant Tumours, 5th ed. New York, NY: Wiley-Liss, 1997, pp 91–97.
21. Travis WD, Colby TV, Corrin B, Shimosato Y, Brambilla E. Historical Typing of Lung and Pleural Tumors, World Health Organization International Histological Classification of Tumors. Berlin: Springer, 1999.
22. Ebright MI, Zakowski MF, Martin J, et al. Clinical pattern and pathologic stage but not histologic features predict outcome for bronchioloalveolar carcinoma. *Ann Thorac Surg* 2002;74:1640–1647.
23. Therasse P, Arbuck SG, Eisenhauer EA, et al. New guidelines to evaluate the response to treatment in solid tumors. European Organization for Research and Treatment of Cancer, National Cancer Institute of the United States, National Cancer Institute of Canada. *J Natl Cancer Inst* 2000;92:205–216.
24. Mellinghoff IK, Wang MY, Vivanco I, et al. Molecular determinants of the response of glioblastomas to EGFR kinase inhibitors. *N Engl J Med* 2006;353:2012–2024.
25. Ohnishi H, Ohtsuka K, Ooide A, et al. A simple and sensitive method for detecting major mutations within the tyrosine kinase domain of the epidermal growth factor receptor gene in non-small-cell lung carcinoma. *Diagn Mol Pathol* 2006;15:101–108.
26. Amann J, Kalyankrishna S, Massion PP, et al. Aberrant epidermal growth factor receptor signaling and enhanced sensitivity to EGFR inhibitors in lung cancer. *Cancer Res* 2006;65:226–235.
27. Ji H, Zhao X, Yuza Y, et al. Epidermal growth factor receptor variant III mutations in lung tumorigenesis and sensitivity to tyrosine kinase inhibitors. *Proc Natl Acad Sci U S A* 2006;103:7817–7822.
28. Kosaka T, Yatabe Y, Endoh H, et al. Mutations of the epidermal growth factor receptor gene in lung cancer: biological and clinical implications. *Cancer Res* 2004;64:8919–8923.
29. Cappuzzo F, Hirsh FR, Rossi E, et al. Epidermal growth factor receptor gene and protein and gefitinib sensitivity in non-small-cell lung cancer. *J Natl Cancer Inst* 2006;97:643–655.
30. Hirsh FR, Varella-Garcia M, Bunn PA Jr, et al. Epidermal growth factor receptor in non-small-cell lung carcinomas: correlation between gene copy number and protein expression and impact on prognosis. *J Clin Oncol* 2003;21:3798–3807.

Size of Metastatic and Nonmetastatic Mediastinal Lymph Nodes in Non-small Cell Lung Cancer

Koei Ikeda, MD, PhD, Hiroaki Nomori, MD, PhD, Takeshi Mori, MD, Hironori Kobayashi, MD, Kazunori Iwatani, MD, and Kentaro Yoshimoto, MD

Objective: To determine the optimum selection of mediastinal lymph nodes for biopsy in non-small cell lung cancer (NSCLC), lymph nodes with or without metastasis at each mediastinal station were ranked in size in patients with pathological N2 disease.

Methods: Twenty-five NSCLC patients with pathological N2 disease who underwent pulmonary resection with complete mediastinal lymph node clearance were examined. Of 114 mediastinal lymph node stations dissected, 47 had metastases and 67 did not. The sizes of 259 nodes in the 47 positive lymph node stations were measured. Of these 259 nodes, 137 had metastases and 122 did not. The short- and long-axis diameters of the 259 lymph nodes were ranked in each lymph node station.

Results: Mean short- and long-axis diameters of lymph nodes with metastases were significantly greater than those without ($p < 0.001$). In 47 metastatic lymph node stations, the short- and long-axis diameters were greatest in a metastatic node in 44 (94%) and 42 (89%) respectively, whereas in the remaining 3 (6%) and 5 (11%), the second largest but not the largest node was positive. None of the largest lymph nodes with metastasis were smaller than the second largest lymph node at each station. Four of the 10 patients with adenocarcinoma (40%) had metastasis in the second largest but not in the largest node measured by long-axis diameter, a significant difference from one in eight (12.5%) among the squamous cell carcinoma cases ($p = 0.04$).

Conclusion: For mediastinal lymph node biopsy, both the largest and the second largest node at each station should be sampled, especially in adenocarcinoma. If only the largest lymph node is selected, false-negative results will occur at a rate of about 10%.

Key Words: Lung cancer, Mediastinal lymph node, Lymph node stage, Sampling, Biopsy.

(*J Thorac Oncol.* 2006;1: 949–952)

Department of Thoracic Surgery, Graduate School of Medicine, Kumamoto University, Kumamoto, Japan.

Address for correspondence: Hiroaki Nomori, MD, PhD, Department of Thoracic Surgery, Graduate School of Medicine, Kumamoto University, Honjo 1-1-1, Kumamoto 860-8556, Japan. E-mail: hnomori@qk9.so-net.ne.jp

ISSN: 1556-0864/06/0109-0949

Although intraoperative N-staging has traditionally been conducted according to the surgeon's experience, Gaer and Goldstraw[1] reported that a naked-eye assessment of nodal staging during lung cancer surgery resulted in 11% false-positive and 9% false-negative assessments. Even for preoperative N-staging, mediastinoscopy and endoscopic ultrasound-guided fine-needle aspiration (EUS-FNA) are reported to have false-negative results,[2–4] which could be attributable to the small size of the biopsy specimens and also to errors in the selection of lymph nodes. Although the largest lymph node is usually selected in mediastinoscopy or EUS-FNA, it has not been confirmed whether the choice of the largest is most appropriate. Thus, it is necessary to consider whether metastasis occurs in the largest lymph nodes. We therefore ranked the sizes of mediastinal lymph nodes with and without metastasis at each nodal station in non-small cell lung cancer (NSCLC) patients with pathological N2 disease.

PATIENTS AND METHODS

Patients

From 1988 to 2005, 420 patients with lung cancer were treated by lobectomy or pneumonectomy with systematic, not lobe-specific, mediastinal lymph node dissection. Of these, 25 patients had mediastinal lymph node metastases (Table 1). Ten patients who underwent neoadjuvant treatment were excluded from the study. Whereas preoperative N-staging was performed by computed tomography (CT) until 2004, positron emission tomography (PET) and EUA-FNA were added for N-staging after 2004. Our treatment strategy for clinical N2 disease was as follows: 1) bulky N2 disease at both superior and inferior mediastinum contraindicated surgery; and 2) N2 disease with multiple affected stations limited to either the superior or inferior mediastinum, or bulky N2 disease at a single station, was treated by neoadjuvant chemoradiotherapy and then surgery.

Pathological Examination

The dissected mediastinal lymph nodes were examined histologically in formalin-fixed paraffin-embedded sections with hematoxylin and eosin (HE) staining. The sections were further examined by immunohistochemical staining with a monoclonal antihuman cytokeratin antibody (DAKO Co., Carpinteria, CA).

TABLE 1. Patient Characteristics

Male	17
Female	8
Mean age (year-old)	63 ± 10
Histological subtype	
Adenocarcinoma	10
Squamous cell carcinoma	8
Adenosquamous carcinoma	2
Large cell carcinoma	4
Mucoepidermoid carcinoma	1
Location of the tumor	
Right upper lobe	11
Right middle lobe	1
Right lower lobe	5
Left upper lobe	6
Left lower lobe	2
Pathological tumor stage	
T1N2M0	6
T2N2M0	13
T3N2M0	3
T4N2M0	3
Total	25

TABLE 2. Lymph Node Nomenclature

N2 Node		N1 Node	
Station	Name	Station	Name
	Superior mediastinal		Hilar
1	Highest mediastinal	10	Hilar
2	Paratracheal	11	Interlobar
3	Pretracheal	12	Lobar
4	Tracheobronchial		Intrapulmonary
	Aortic	13	Segmental
5	Botallo	14	Subsegmental
6	Para-aortic		
	Inferior mediastinal		
7	Subcarinal		
8	Paraesophageal		
9	Pulmonary ligament		

Lymph Node Stations

The lymph node nomenclature used was from the lymph node map of Naruke et al,[5] as approved by The Japan Lung Cancer Society (Table 2).

Measurement of Lymph Node Size

The short- and long-axis diameters of all lymph nodes were measured on HE-stained sections and ranked for each lymph node station.

Statistical Analysis

All data were analyzed for significance using two-tailed Student's t tests or χ^2 tests. Differences at $p < 0.05$ were accepted as significant. All values in the text and tables are given as mean ± SD.

TABLE 3. Number of Mediastinal Lymph Node Stations with Metastasis in Each Lobe

Lobe	Superior Mediastinum	Inferior Mediastinum (#7)	Total
Right upper lobe	24	2	26
Right middle lobe	0	1	1
Right lower lobe	5	1	6
Left upper lobe	12	0	12
Left lower lobe	1	1	2
Total	42	5	47

TABLE 4. Size of the Lymph Nodes with or Without Metastasis in the Metastatic Lymph Node Stations

	Lymph Nodes		
	With Metastasis	Without Metastasis	p Value
Number	137	122	
Short-axis diameter (mm)			$p < 0.001$
Mean	5 ± 3	3 ± 2	
Range	0.5–18	0.5–11	
Long-axis diameter (mm)			$p < 0.001$
Mean	8 ± 5	5 ± 3	
Range	0.5–33	0.5–19	

RESULTS

A total of 114 mediastinal lymph node stations were resected in 25 patients. Of these, 47 stations had metastatic lymph nodes and 67 did not. Whereas 13 of the 25 patients had metastases at a single nodal station, the other 12 had metastases at multiple stations. Table 3 shows the distribution of the 47 metastatic lymph node stations in each lobe. Whereas tumors in the upper lobes had metastases almost in the superior mediastinum, tumors in the right lower lobe did not show the uniform distribution of metastases, that is, four of the five tumors had single-station metastasis in the superior mediastinum, and the remaining one had metastases in both the superior and inferior mediastinum. In the 47 lymph node stations containing metastases, there were 137 lymph nodes with metastases and 122 without (Table 4). Among the 137 metastatic lymph nodes, micrometastasis was found in three (2%) by immunohistochemical examination. The mean short-axis diameter of the lymph nodes with metastasis was 5 ± 3 mm, which was significantly larger than that of those without metastasis (3 ± 2 mm; $p < 0.001$). The mean long-axis diameter of lymph nodes with metastasis was 8 ± 5 mm, which was significantly greater than that of those without metastasis (5 ± 3 mm; $p < 0.001$).

Table 5 shows a ranking of the largest lymph nodes with metastasis at each lymph node station. By short-axis diameter, the largest lymph node had metastases in 44 of the

TABLE 5. Rank of the Size of Lymph Nodes with Metastasis in Each Lymph Node Station

Measured by Short-Axis Diameter	
Largest lymph node	44
Second largest lymph node	3
Smaller than the second one	0
Measured by long-axis diameter	
Largest lymph node	42
Second largest lymph node	5
Smaller than the second	0
Total	47

47 affected lymph node stations (94%). In the remaining three lymph node stations (6%), the largest lymph node was clear of metastasis, but the second largest had metastasis. By long-axis diameter, the largest lymph node had metastasis in 42 of the 47 stations (89%), and in the remaining five lymph node stations (11%), the second largest lymph node was involved, but the largest was not. None of the largest lymph nodes with metastasis were smaller than the second largest one in any of the stations when measuring both the short- and long-axis diameters. Four of 10 patients with adenocarcinoma (40%) had metastasis in the second largest lymph node as measured by long-axis diameter, but not in the largest one, which was more common than in squamous cell carcinoma, where this occurred in one of eight cases (12.5%) ($p = 0.04$).

DISCUSSION

The present study has demonstrated the following points: 1) In pathological N2 disease, approximately 90% of metastases were found in the largest lymph node at its nodal station; 2) approximately 10% of metastasis were in the second largest but not in the largest lymph node of each station; 3) none of the metastatic lymph nodes were smaller than the second largest lymph node of any nodal station; and 4) adenocarcinoma had metastasis in the second largest lymph node, but not in the largest lymph node, more frequently than squamous cell carcinoma. Therefore, examining both the largest and second largest lymph nodes is necessary to reach 100% sensitivity for preoperative and intraoperative mediastinal lymph node staging. However, it should be kept in mind that the present study measured the sizes of lymph nodes in fixed, cut, and stained specimens, which were smaller than their size at the moment of preoperative or intraoperative nodal evaluation. Therefore, the absolute sizes of lymph nodes shown in Table 5 are not applicable to preoperative or intraoperative evaluation of lymph nodes. The present study is concerned with the rank order of sizes of metastatic mediastinal lymph nodes at each nodal station.

It is well known that systematic mediastinal lymph node dissection does not increase postoperative morbidity or mortality.[6,7] However, the recent increase of clinical stage Ia NSCLC has led to increased use of limited lung resection as well as a reduction in mediastinal lymph node dissection. Segmentectomy has been reported to have a similar postoperative prognosis as lobectomy when intraoperative frozen sections of hilar and mediastinal lymph nodes show no metastasis.[8] Whereas the International Association for the Study of Lung Cancer Staging Committee has determined that the definition of stage p-N0 should be based on the pathological findings of systematic mediastinal lymph node dissection,[9] several authors have proposed lobe-specific mediastinal lymph node dissection for patients with clinical stage Ia NSCLC to minimize surgical damage[10–13]; that is, the dissection of inferior mediastinal lymph node stations could be reduced for upper lobectomy when the hilar and superior mediastinal lymph nodes are negative for metastases, and the dissection of superior mediastinal lymph node stations could be reduced for lower lobectomy when the hilar and inferior mediastinal lymph nodes are negative for malignancy. However, before the final decision is made on both segmentectomy and lobe-specific mediastinal lymph node dissection, a large number of lymph nodes need to be submitted for intraoperative frozen section. To reduce the number of lymph nodes required for this, several authors have proposed intraoperative sentinel lymph node biopsy using radioisotopes.[14–16] However, this necessitates preoperative injection of radioisotopes and intraoperative measurement of the radioactivity of lymph nodes. Based on the results of the present study, we believe that taking the largest and the second largest lymph nodes at each station would provide a sufficient sample of intraoperative frozen sections and would minimize the number of intraoperative frozen sections taken.

Which lymph node stations should be submitted for intraoperative frozen section during lung cancer surgery? In 1999, Naruke et al[10] examined the distribution of lymph node metastasis (i.e., sentinel nodes) in each lobe from data on 1815 patients with T1 NSCLC who had major lung resection with mediastinal lymph node dissection. They concluded that, whereas hilar lymph nodes were usually sentinel nodes in lung cancer, the following mediastinal lymph nodes could be sentinel nodes: #3 and/or #4 in the right upper lobe, #3 and/or #7 in the right middle lobe, #7 in the right lower lobe, #5 and/or #6 in the left upper lobe, and #7 in the left lower lobe. Other authors have reported similar results.[17,18] The present study, however, although showing similar results for the upper lobes of both sides, demonstrated that four of five lung cancers in the right lower lobe had a single metastasis at station #3 or #4. According to our previous study of sentinel node identification using ^{99m}Tc-tin colloid, two of eight NSCLC in the right lower lobe had sentinel nodes in both #4 and #7.[15] We consider that the lymphatic flow from the right lower lobe could partly drain to the superior mediastinum (#3 and #4) along the main bronchus. From the previous report and from the present study, a plan for efficient intraoperative N-staging could be as follows: hilar lymph nodes and lobe-specific mediastinal lymph nodes are dissected;, and the largest and second largest lymph nodes from each station are submitted for intraoperative frozen section. In this way, the number of lymph nodes for frozen section would be minimized.

Although mediastinoscopy and EUS-FNA have been proposed for mediastinal lymph node biopsy, they are known to have false-negative results.[2–4] EUS-FNA is now the least invasive procedure for pathological or cytological diagnosis